DR2004167

APPENDIX ON PALEOMAGNETIC ANALYSES

Samples were stored, thermally demagnetized, and measured in a magnetically shielded room with average field intensity <200 nT. After measurement of natural remanent magnetization (NRM), thermal demagnetization at 18 temperature steps up to 600°C was performed on two pilot samples from each site. Typical thermal-demagnetization behaviors are illustrated in Figure DR2[1]. Minor directional changes were observed at temperatures less than 300°C. At higher temperatures, a characteristic remanent magnetization (ChRM) was isolated with unblocking temperatures up to 580°C. Remaining samples were demagnetized at ≥ eight temperatures concentrated within the unblocking temperature interval of the ChRM. Sample directions of ChRM were determined by principal component analysis (Kirschvink, 1980) and ChRM directions with maximum angular deviation (MAD) ≤15° were retained for further analysis. Using Fisher (1953) statistics, sample ChRM directions were averaged to determine the site-mean directions. Sample ChRM directions more than two angular standard deviations from the initial site-mean direction were not used to calculate the final site-mean direction. The resulting 72 site-mean directions with 95% confidence limit (α_{95}) ≤ 15° are listed in Table DR1[1]. Samples from 23 sites failed to yield acceptable site-mean directions.

Site-mean ChRM directions are equally divided between normal and reversed polarities. The mean direction from the normal polarity sites is inclination (I) = 69.5° and declination (D) = 28.0° (α_{95} = 5.9°; N=36; k = 17.5) while the mean direction from the reverse polarity sites is I = -70.6° and D = 230.9° (α_{95} = 4.8°; N=36; k = 25.6). These directions pass the reversal test with class B designation (McFadden and McElhinny, 1990). Inverting reversed polarity site-mean directions and computing the overall mean direction yields I = 70.4°; D = 39.3° (α_{95} = 4.8°; N= 72; k = 20.1). Using the Oligocene reference paleomagnetic pole at 84.0°N, 168.0°E, A_{95} = 4.0° (Diehl et al., 1988), the expected direction is: I = 73.3° ± 2.5°; D = 350.0° ± 7.8°. Applying the methods of Beck (1980) and Demarest (1983) to compare the observed and expected directions yields inclination flattening (F ± ΔF) of 2.9° ± 4.3° and rotation of declination (D ± ΔD) of 49.3° ± 13.1°. Using the Miocene reference pole at 87.4°N, 129.7°E, A_{95} = 3.0° (Hagstrum et al., 1987), the expected Miocene direction only differs from the expected Oligocene direction by ~2°, so the choice of reference pole has negligible effect on the paleomagnetic discordance.

REFERENCES CITED

Beck, M. E., Jr., 1980, Paleomagnetic record of plate-margin tectonic processes along the western edge of North America: Journal of Geophysical Research, v. 85, p. 7115–7131.

Demarest, H. H., 1983, Error analysis of the determination of tectonic rotations from paleomagnetic data: Journal of Geophysical Research, v. 88, p. 4321–4328.

Diehl, J. F., McClannahan, K. M., and Bornhorst, T. J., 1988, Paleomagnetic results from the Mogollon-Datil volcanic field, southwestern New Mexico, and a refined mid-Tertiary reference pole for North America: Journal of Geophysical Research, v. 93, p. 4869-4879.

Fisher, R. A., 1953, Dispersion on a sphere: Royal Society of London Proceedings, v. A217, p. 295–305.

Hagstrum, J. T., Sawlan, M. G., Hausback, B. P., Smith, J. G., and Grommé, C. S., 1987, Miocene paleomagnetism and tectonic setting of the Baja California Peninsula, Mexico: Journal of Geophysical Research, v. 92, p. 2627-2639.
Kirschvink, J. L., 1980, The least-square line and plane and the analysis of paleomagnetic data: Royal Astronomical Society Geophysical Journal, v. 62, p. 699–718.
McFadden, P. L., and McElhinny, M. W., 1990, Classification of the reversal test in palaeomagnetism: Geophysical Journal International, v. 103, p. 725–729.

TABLE DR1. SITE-MEAN DIRECTIONS OF CHARACTERISTIC MAGNETIZATION

Site No.	Lat. N	Long. W	N	k	J (10^{-2} A/m)	α_{95} (°)	I (°)	D (°)
Conclusion Island								
WT226	56° 29.017'	133° 50.044'	8	210.0	17.0	3.8	-79.1	203.5
WT227	56° 28.897'	133° 49.854'	6	166.1	19.0	5.2	-86.2	186.3
Monte Carlo Islands								
WT229	56° 31.874'	133° 46.695'	6	157.8	82.0	5.3	-63.1	260.2
WT230	56° 31.874'	133° 46.695'	7	104.8	2.7	5.9	-63.1	251.0
WT231	56° 31.965'	133° 46.615'	8	50.5	1.8	7.9	-68.3	246.5
WT232	56° 32.010'	133° 46.481'	7	145.8	37.0	5.0	-56.3	251.6
WT233	56° 32.060'	133° 46.429'	8	450.2	95.0	2.6	-64.1	238.9
Three Mile Arm								
WT236	56° 35.228'	133° 51.826'	5	66.7	0.6	9.4	-75.4	176.5
WT237	56° 35.246'	133° 51.887'	7	264.8	10.0	3.7	81.3	134.6
WT239	56° 35.757'	133° 52.387'	7	24.2	5.3	12.5	75.9	0.1
WT240	56° 35.716'	133° 52.446'	5	114.3	6.1	7.2	73.5	336.8
WT243	56° 35.965'	133° 53.186'	8	50.5	15.0	7.9	75.4	240.1
WT244	56° 36.390'	133° 53.724'	6	129.1	0.8	5.9	62.2	18.7
WT245	56° 36.390'	133° 53.724'	8	215.3	40.0	3.8	79.5	328.0
WT246	56° 32.653'	133° 50.746'	8	59.5	35.0	7.2	37.7	20.2
WT248	56° 28.764'	133° 52.530'	6	97.4	14.0	6.8	87.5	71.4
Kupreanof Island								
WT515	56° 25.600'	133° 38.101'	8	554.3	31.0	2.4	-81.5	80.7
WT516	56° 26.063'	133° 37.796'	8	276.4	62.0	3.3	-65.7	163.6
WT520	56° 25.205'	133° 30.987'	8	156.1	39.0	4.4	-83.3	294.6
WT524	56° 27.217'	133° 14.195'	6	145.5	11.0	5.6	53.5	339.2
WT525	56° 26.833'	133° 13.593'	7	53.9	30.0	8.3	69.0	323.0
WT526	56° 26.637'	133° 12.679'	5	99.6	18.0	7.7	51.9	334.7
WT527	56° 26.839'	133° 12.241'	9	265.4	11.0	3.2	65.1	350.0
WT530	56° 26.984'	133° 06.708'	7	81.5	17.0	6.7	56.9	37.1
Zarembo Island								
WT004	56° 27.385'	132° 52.234'	7	393.8	40.0	3.0	-68.4	222.2
WT018	56° 19.000'	133° 02.056'	7	70.3	2.9	7.2	-59.1	197.3
WT020	56° 19.000'	133° 02.056'	6	927.7	26.0	2.2	-71.5	271.9
WT021	56° 19.153'	133° 02.639'	5	654.3	31.0	3.0	-83.4	4.5
WT024	56° 19.998'	133° 03.973'	5	149.5	11.0	6.3	-61.6	168.1
WT025	56° 22.150'	133° 03.189'	5	525.5	9.1	3.3	-35.4	297.2
WT026	56° 22.796'	133° 02 701'	7	47.5	9.2	8.9	27.1	32.0

WT027	56° 22.796'	133° 02 701'	6	49.0	54.0	9.7	70.9	47.1
WT097	56° 14.622'	132° 49.054'	6	63.5	8.5	8.5	59.9	39.8
WT098	56° 14.622'	132° 49.054'	5	621.2	17.0	3.1	45.8	17.2
WT099	56° 14.622'	132° 49.054'	6	459.7	37.0	3.1	61.6	64.9
WT100	56° 14.622'	132° 49.054'	6	498.5	41.0	3.0	61.4	68.3
WT101	56° 14.009'	132° 51.389'	6	643.9	61.0	2.6	-69.5	235.0
WT102	56° 14.009'	132° 51.389'	6	121.8	6.5	6.1	-75.7	208.5
WT104	56° 14.009'	132° 51.389'	6	328.8	24.0	3.7	-71.4	259.1
WT276	56° 26.981'	132° 58.435'	7	74.0	21.0	7.1	47.5	14.6
WT278	56° 27.374'	132° 52.338'	5	108.8	21.0	7.4	-57.8	247.5
WT281	56° 27.149'	132° 51.463'	6	226.2	44.0	4.5	-50.3	253.2
WT283	56° 26.999'	132° 51.042'	7	111.2	15.0	5.7	-65.1	242.9
WT288	56° 26.473'	132° 49.147'	6	194.2	2.6	4.8	-75.8	268.4
WT289	56° 26.473'	132° 49.147'	4	47.1	1.2	13.5	-77.3	241.4
WT426	56° 14.213'	132° 50.798'	7	70.1	37.0	7.3	-58.6	221.0
WT427	56° 14.213'	132° 50.798'	8	236.8	46.0	3.6	49.0	74.5
WT428	56° 14.213'	132° 50.798'	8	271.5	29.0	3.4	-71.7	229.7
WT429	56° 14.213'	132° 50.798'	5	98.5	9.9	7.7	44.6	91.3
WT430	56° 14.213'	132° 50.798'	7	527.9	2.7	2.6	-53.6	240.7
WT431	56° 14.382'	132° 50.337'	6	353.6	88.0	3.6	-55.0	207.3
WT433	56° 14.382'	132° 50.337'	6	155.9	89.0	5.4	67.0	24.6
WT434	56° 14.382'	132° 50.337'	7	233.2	310.0	4.0	65.5	11.1
WT435	56° 14.382'	132° 50.337'	7	124.1	93.0	5.4	65.2	30.4
WT438	56° 14.382'	132° 50.337'	5	29.6	34.0	14.3	69.6	86.5
WT531	56° 16.283'	132° 40.468'	8	208.3	190.0	3.8	73.9	20.3
WT532	56° 16.283'	132° 40.468'	8	425.9	220.0	2.7	78.9	337.2
WT533	56° 15.719'	132° 42.417'	8	180.3	39.0	4.1	67.1	16.7
WT534	56° 15.817'	132° 41.420'	8	573.9	62.0	2.3	-51.4	233.5
WT536	56° 15.087'	132° 45.959'	4	1.9	1.5	94.1	-53.4	222.9
Deer Island								
WT074	56° 03.000'	132° 03.897'	7	239.0	12.0	3.9	56.6	59.6
WT406	56° 02.617'	131° 59.600'	6	830.8	3.8	2.3	-73.2	204.5
WT412	56° 02.541'	132° 03.342'	7	172.8	1.1	4.6	67.8	78.1
WT420	55° 58.947'	132° 02.839'	4	371.8	4.5	4.8	-49.6	215.3
WT423	56° 01.473'	132° 04.135'	5	92.6	0.4	8.0	-52.4	237.6
Etolin Island								
WT078	56° 07.077'	132° 14.634'	7	168.3	2.8	4.7	72.5	348.8
WT092	56° 14.501'	132° 37.651'	6	779.7	41.0	2.4	66.8	27.6
WT093	56° 14.501'	132° 37.651'	6	375.6	65.0	3.5	67.0	34.0
WT537	56° 14.118'	132° 39.266'	8	105.8	380.0	5.4	64.8	24.6
WT539	56° 14.037'	132° 38.379'	8	263.7	16.0	3.4	81.1	349.0
WT540	56° 14.271'	132° 36.518'	8	171.8	4.6	4.2	-71.3	207.3
Wrangell Island								

WT305	56° 17.908'	131°	59.836'	6	153.8	12.0	5.4	-75.5	231.2

Notes: Site No. - Paleomagnetic site number; N – number of samples used to determine site-mean direction; J – geometric mean intensity of characteristic remanent magnetization (component remaining after removal of secondary components during thermal demagnetization); α_{95} - radius of cone of 95% confidence about site-mean direction; k – best-estimate of Fisher precision parameter; I and D - inclination and declination of site-mean direction.

DRFigCaps.doc

Figure DR1. Whole rock $^{40}Ar/^{39}Ar$ release spectra and isochron diagrams of mafic dikes. **A**. Site WT277 from Zarembo Island. **B**. Site WT305 from Wrangell Island.

Figure DR2. Vector-component diagrams of thermal demagnetization behavior. **A**. Reversed-polarity sample. **B**. Normal-polarity sample. Open circles—projections onto vertical plane; filled circles—projections onto horizontal plane. Numbers adjacent to data points indicate temperatures (in °C).

Figure DR1 Butzer et al.

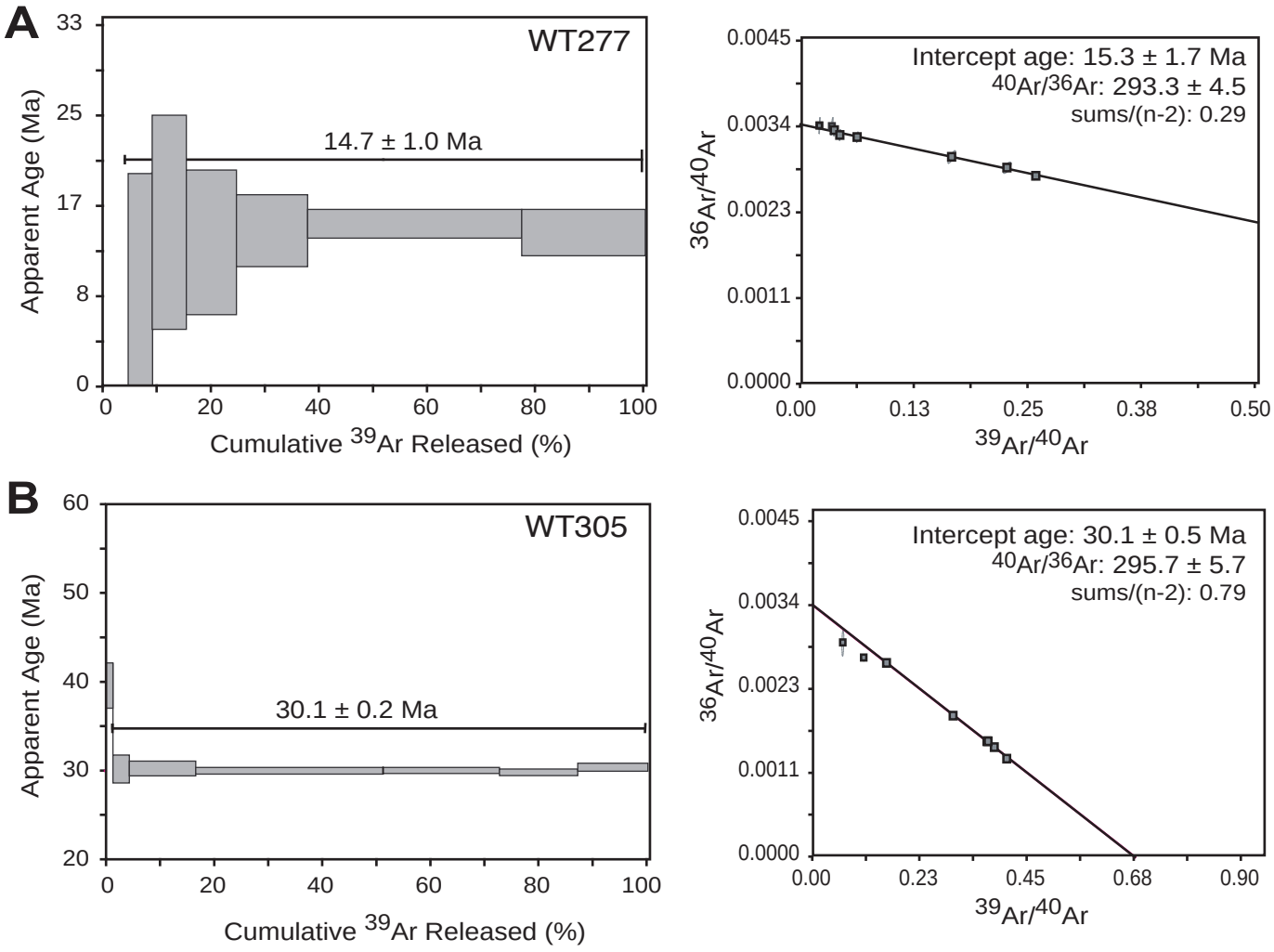

Figure DR2, Butzer et al.